Correlation of photoluminescence and symmetry studies with photoexcitation and decay processes of infrared active defects in Si

W. J. Vidinski,[a] A. J. Steckl,[b] and J. C. Corelli[c]
Center for Integrated Electronics, Rensselaer Polytechnic Institute, Troy, New York 12181

(Received 31 January 1983; accepted for publication 25 March 1983)

Defects introduced in silicon by neutrons and ions which give rise to infrared active electronic defect absorption bands after heat treatment to 500 °C were studied using a dual beam optical method. The measurements were made in the 11–90 K temperature range on four defect bands found in the 900 (11.1)–1100 cm^{-1} (9.09 μm) region of the infrared spectrum. The studies yield results on the capture cross sections of photoexcited electrons from defects which lead to a model of a defect having three different charge states. These cross sections are much smaller than those reported for the photoionization cross sections of chemical impurities such as Au in silicon. The states found in this study can be identified with photoluminescence peaks reported by others near 1 and 0.76 eV. Additionally, there are two different symmetries assumed by the defects responsible for the defect absorption bands.

PACS numbers: 78.50.Ge, 61.80.Hg, 61.70.Bv, 81.40.Tv

INTRODUCTION

The defects created by fast neutron irradiation are closely related to those introduced during the fabrication of silicon devices and integrated circuits, for example, by neutron transmutation doping or ion implantation with subsequent high temperature annealing. In addition to microstructural defects such as dislocations, vacancy dislocation loops, stacking faults, voids, and "rod-like defects," many defects are electrically and optically active prior to heat treatment ~850 °C. The optically active defects manifest themselves as either impurity associated (e.g., C,O) infrared vibrational absorption bands or electronic infrared-active defect absorption bands.

In this paper we shall focus on several of the electronic bands which appear only after the irradiated silicon material is heat treated for ~20 min at 400–600 °C. The total number of such observed sharp absorption bands is found to be as high as 26 and their fluence, annealing, and impurity dependence have been studied by others in the past decade.[1–7] These bands which are found in the 6–15 μm wavelength region, have been designated, as higher order bands (HOB)[3] since they are due to defect complexes formed only after the disappearance of the simpler point defects like for example divacancies.

During the past 25 years there have been at least 114 different defect absorption bands observed in irradiated silicon which have been documented in the literature. A summary of the reported defect absorption bands induced by neutrons, ions, and electrons of energy $\geqslant$2 MeV is given elsewhere.[8] It is important to note that detailed microscopic models of the defects which give rise to these absorption bands have been given for only a small number of this class of infrared active defect centers.

EXPERIMENTAL METHODS

The method we use to study the infrared active electronic defect absorption bands involves the illumination of the sample simultaneously with two monochromatic light beams of specific energy and is based on the fact that there must be electrons present in the ground state of the defect in order to observe the optical transition giving rise to the HOB absorption bands. This is accomplished experimentally by two monochromators. One monochromator supplies a beam at wavelength λ_e and energy E_e (excitation light) to pump electrons from the valence band to the defect center, while at the same time a second monochromator illuminates the sample with a second beam of wavelength λ_p (probe light) tuned to the transition energy of the particular defect absorption band. The absorption of the probe beam by the sample is subsequently detected and recorded as the sample temperature and excitation energy is varied. The resultant data yields information on photoexcitation electron capture cross section versus excitation energy, capture cross section versus temperature, and photoexcitation and decay times versus temperature for the particular defect. From such studies one can gain insight into the nature of irradiation-induced defects using a probe which gives different information than provided for example by measurements of electrical properties, photoconductivity, deep level transient spectroscopy, and electron paramagnetic resonance.

The samples studied were cut from n-type float zone refined silicon phosphorus doped to $\cong$170 Ω cm and irradiated to fast neutron fluences up to 10^{18} cm^{-2} ($E>1$ MeV) and thermal neutron fluences up to 6×10^{18} cm^{-2}. During irradiation in the Bulk Shielding Reactor at the Oak Ridge Laboratory the sample temperature was held near 50 °C. The ingots were cut to dimensions 2.5 by 2.5 cm and 3 mm, and the two faces were fine polished to a mirror-like finish. Since it is necessary to heat treat a sample in order to observe higher order bands, a 500 °C anneal in air for 15 min was performed on each sample before mounting within the cryostat.

[a] Now at Ft. Huachuca, Arizona.
[b] Department of Electrical, Computer and Systems Engineering.
[c] Department of Nuclear Engineering.

 0021-8979/83/074097-07$02.40

An Air Products LT-3-110 Helitran Cryostat was used to attain sample temperatures in the range $11 \lesssim T \lesssim 100$ K. The cryostat housing contained three Irtran II windows for entry/exit of the probe beam and entry of the excitation beam. A mechanical shutter with a speed of 1/100 s controlled the entry of the excitation beam. Further precautions were taken to ensure that the experiments were conducted under background light-excluded conditions.

The excitation beam was provided by a Perkin–Elmer Model 98 monochromator with fused silica prism. The probe beam was provided by a Spex Model 1700-3 3/4-m Czerny–Turner diffraction grating spectrometer. Both monochromators were instrumented with suitable optics such as prisms and diffraction gratings to cover the wavelength range 1–14 μm. Detection of the relative intensity of the probe light transmitted through the sample was accomplished by standard low noise preamplifier and lock-in amplifier electronics. Additional details of the experimental methods used in our studies can be found elsewhere.[9,10]

The optical configuration of the two monochromators is such that both the probe and excitation light beams which are 90° with respect to each other impinge coincidentally upon the sample. In addition, the probe beam strikes the sample surface at approximately 30° from normal incidence. Provision is made to eliminate all stray light from illuminating the sample.

The basic experiment consisted of applying to the sample a step of monochromatic light with the excitation beam while simultaneously illuminating the sample with light of wavelength corresponding to a specific defect absorption band until steady-state absorption was reached. During this period the absorption of the probe beam at the specific defect band was monitored and recorded. The excitation step was then removed, while again the probe beam absorption was recorded. Temperature, probe and excitation energies were held constant as the sample went from one steady-state condition to the other. Since the photoexcitation capture cross section is proportional to the probe beam absorption difference between initial and final steady states, the capture cross section versus excitation energy was obtained by normalizing the difference to the output power of the excitation source for different wavelengths of excitation energy. A family of cross-section curves can be constructed for the given defect band (λ_p = constant) by repeating this procedure at different temperatures.

RESULTS

In Fig. 1 is shown a typical plot of the probe detector response tuned to the 1048 cm^{-1} (9.54 μm) HOB. For this band the sample temperature was 15 K and the excitation light energy was $E_e = 1.33$ eV. The time constants are defined on Fig. 1; i.e., τ_e^1 is the fast excitation time, T_e^2 the (longer) second excitation time, τ_d^1 the fast decay time accompanied by a much slower decay time.

The transitions giving rise to the absorption in the 1048 cm^{-1} band commence when the excitation light is turned on. A decrease in the absorption commences when the excitation light is turned off. In order to enhance the decay (empty states of electrons) we have found that illuminating the sample with what we call the depletion energy of 0.74 eV quickly restores the state to its original condition (empty of electrons)

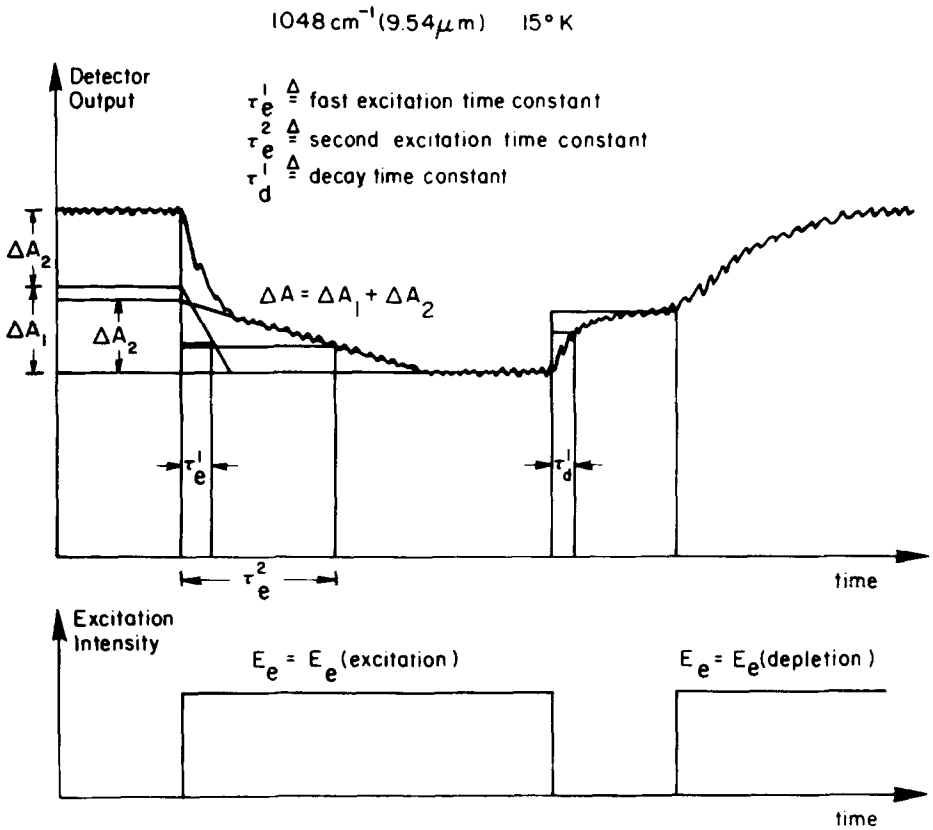

FIG. 1. Time dependence of the photoexcitation and decay of the 1048 cm^{-1} (9.54 μm) HOB. The excitation energy was $E_e = 1.33$ eV, the depletion energy was $E_e = 0.74$ eV, and the sample temperature was 15 K.

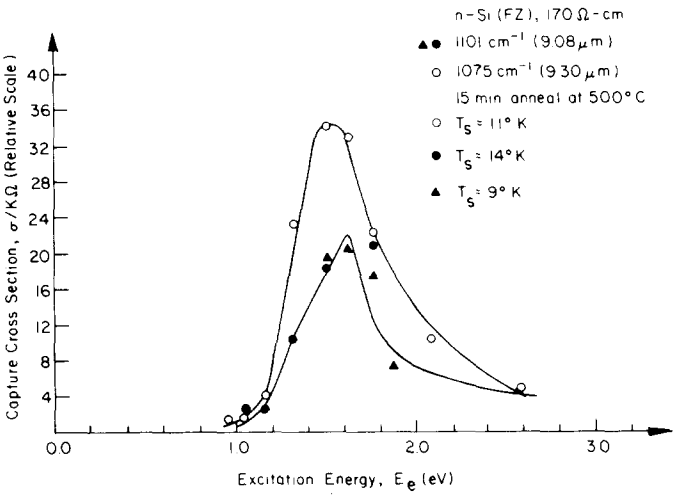

FIG. 2. Capture cross section vs excitation for the 1101 and 1075 cm^{-1} HOB at 9, 11, and 14 K.

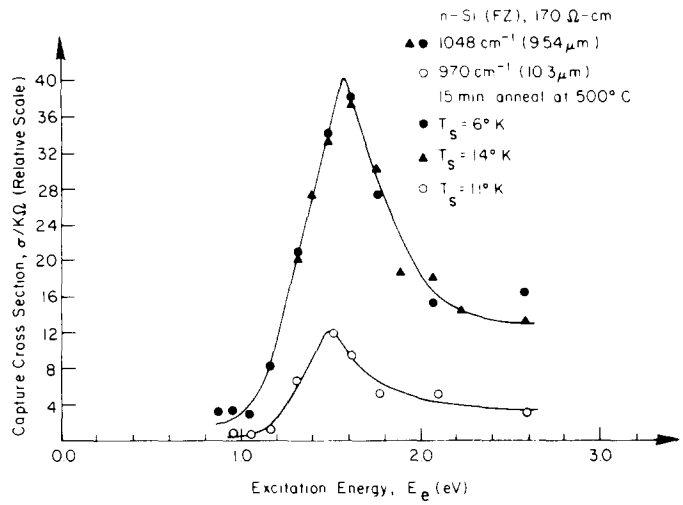

FIG. 3. Capture cross section vs excitation for the 1148 and 970 cm^{-1} HOB at 6, 11, and 14 K.

as can be seen in Fig. 1. We can also empty the state of electrons by subjecting the sample to a short ($\sim$20 s) heat pulse which raises the sample temperature to $\sim$250 K. The significance of the depletion energy will be discussed further in the context of the model we propose for the defect states.

The results shown in Fig. 1 are the most complex photoexcitation and decay processes we have observed in that some of the HOB we have studied only exhibit a single excitation and a single decay time, whereas, other HOB exhibit at least two excitation and two decay times. These additional results are given elsewhere.[10] We do not observe any sample thickness or surface treatment effects on HOB. In general, we find if there are two decay times the short one occurs for times <15 s while the long-lived decay can be $\geq$30 min in duration.

In Figs. 2 and 3 we show results giving the electron capture cross section of photoexcited electrons as a function of the photoexcitation energy for the 1101, 1075 (Fig. 2), and 1048, 970 cm^{-1} (Fig. 3) HOB studied in this investigation. The sample temperature was kept constant in the 6–14 K range for the measurements in Figs. 2 and 3. The capture cross sections are normalized to the relative incident flux of photons from the spectrum emitted by the excitation light source monochromator. The signal difference between initial and final state (Fig. 1) is assumed to be proportional to the cross section and all electronic parameters such as amplifier gain, integration time constant are kept fixed as the excitation energy is varied. Each cross section displays a characteristic maximum near 1.55 ± 0.05 eV. The attenuation coefficient in silicon for the light in the 1.2- and 2.2-eV range is such that most of the photoexcited electrons are produced within 10 μm of the sample surface.[11]

In Fig. 4 is shown the temperature dependence of the capture cross section for the 1075 cm^{-1} HOB for incident excitation energy near the maximum 1.49 eV. Note that the capture cross section is nearly constant showing only a slight increase from $\sim$10 to 65 K followed by a decrease above 65 K. This temperature dependence is markedly different than

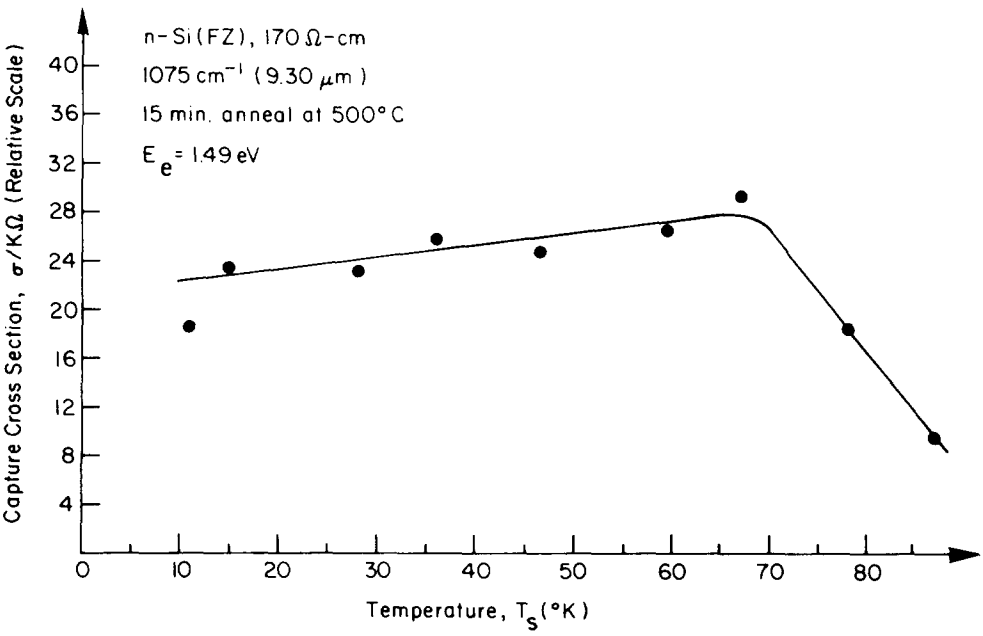

FIG. 4. Capture cross section vs temperature for the 1075 cm^{-1} HOB using 1.49-eV excitation energy.

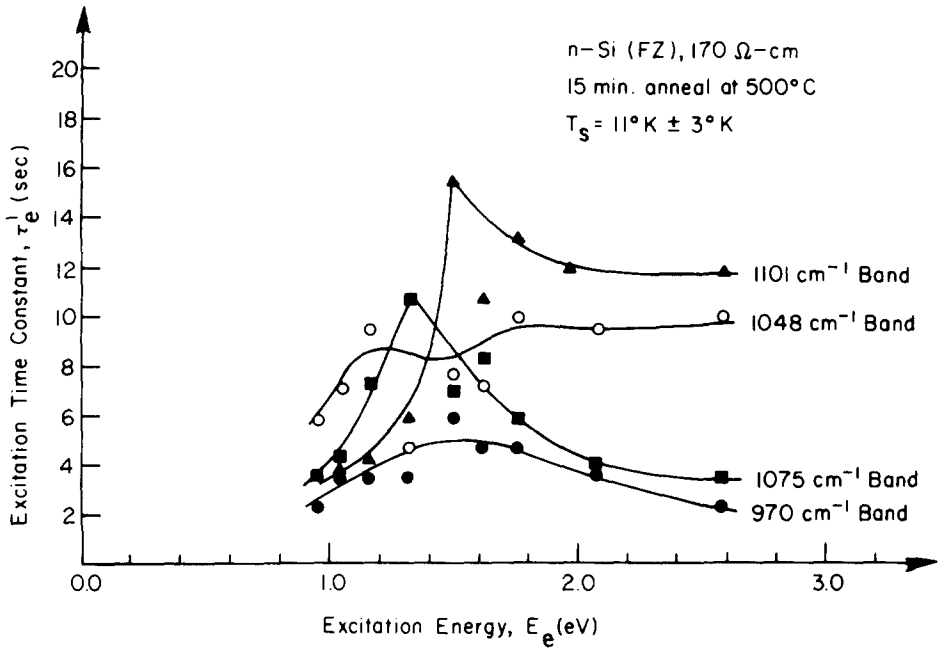

FIG. 5. Excitation time constants vs excitation energy at constant temperature.

that found for the divacancy-associated 2762 cm^{-1} (3.62 μm) band[10] for which the capture cross section is constant from 30 to 90 K and then rises sharply at temperatures below 30 K.

A summary of the dependence of the excitation time constants on the excitation energy is given in Fig. 5 while similar results for the decay constants are given in Fig. 6 for the HOB studied. The sample temperature was kept at 11 ± 3 K during the measurements. The time constants are defined as the time to reach $1/e$ of the absorption mode (excitation time τ_e^1). The decay time constant τ_d^1 is defined as the time to reach $1/e$ of the initial state (no absorption). Figure 7 is a plot showing the temperature dependence of the excitation and decay time constants for the 1075 cm^{-1} HOB determined with an excitation energy of 1.49 eV. As can be seen in Fig. 7 the initial excitation τ_e^1 and initial decay times τ_d^1 are in the range 4–8 s and are independent of temperature.

DISCUSSION OF RESULTS AND CONCLUSIONS

A. Energy state model of HOB

The defect giving rise to the HOB studied has three different charge states within the bandgap of silicon as was proposed previously.[8,9] The charge states are T, T^*, and T^{**} shown in Fig. 8(a). As the defect center captures successive electrons it is promoted to the next higher charge state. The energy level positions are as shown in Fig. 8(a). We conclude that the process can be described as

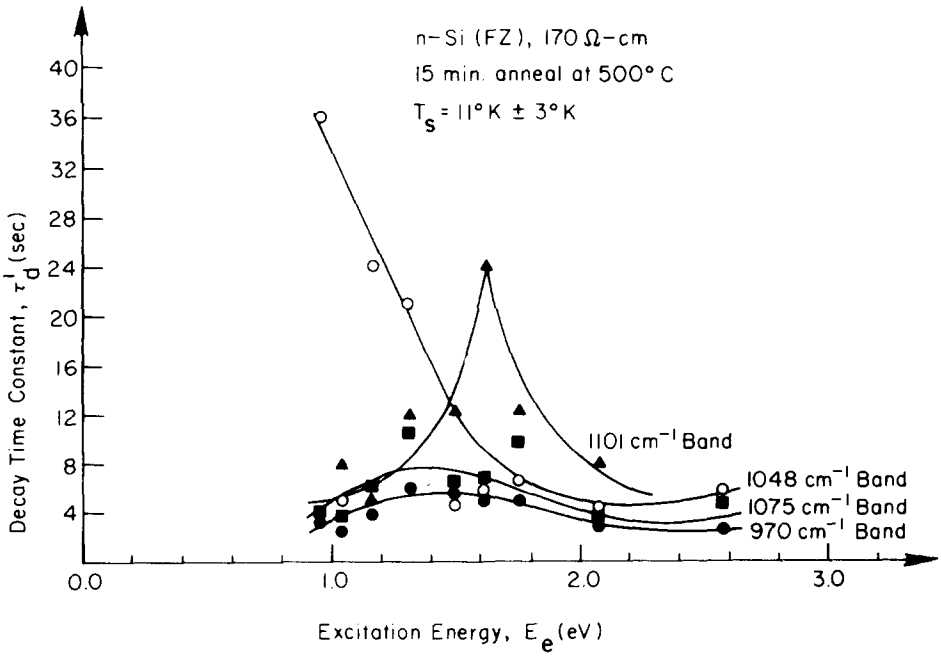

FIG. 6. Decay time constants vs excitation energy at constant temperature.

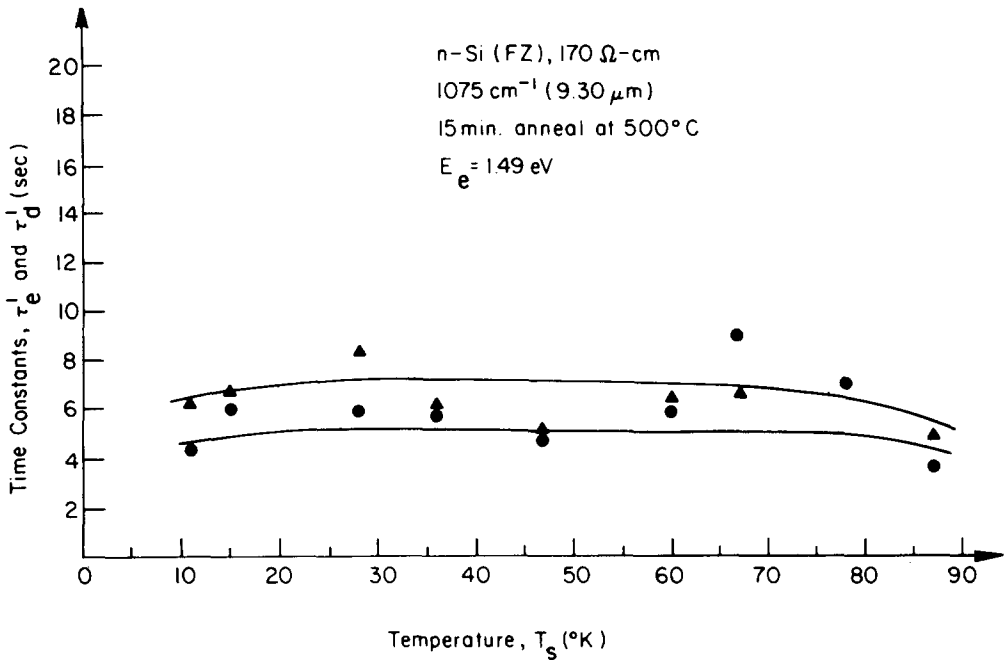

FIG. 7. Excitation ● and decay ▲ time constants vs temperature for the 1075 cm^{-1} HOB using 1.49-eV excitation light.

$$T + e^- \rightleftarrows T^*,$$

and

$$T^* + e^- \rightleftarrows T^{**},$$

where T represents the empty defect state located ~ 0.17 eV above the valence band, T^* the intermediate defect state after capture of one electron located 0.42 eV above the valence band, and T^{**} the defect state (energy location < 0.72 eV below conduction band) after capture of two electrons from which the optical transition of the HOB takes place. The source of these electrons are the conduction band electrons optically excited from the valence band by the excitation beam with energy $E_e \pm \Delta E_e$. Simultaneously, the probe beam (λ_p) with energy $E_p \pm \Delta E_p$ is tuned to the absorption energy of one of the HOB. Increased absorption of the probe beam occurs as the defect centers are increasingly populated with electrons captured from the conduction band [Fig. 8(b)], and this increased absorption is a measure of the fraction of defect centers in the T^{**} change state. The additional probe beam absorption (with excitation light turned off Fig. 1) implies that there are defect centers existing in both the T^* and T^{**} charge states. In earlier work[8,9] it was recognized that the T^* charge state must be a relatively strong trapping center. Upon removal of the excitation source [Fig. 8(c)], it is assumed that T^{**} decays to T^* [Fig. 8(c)]. However, as can be seen in Fig. 1 the probe beam absorption does not return to its original level after the decay process is completed (see Fig. 1). Additionally the energy width of the probe beam ΔE_p [$\leqslant 0.005$ eV) may be such that the probe beam may also excite an energy state of the T^* charge state which is equal or nearly equal to that of the T^{**} charge state. Moreover, it is reasonable to postulate that the energy configuration of the defect center may be such that its configuration is less effective in absorbing the probe beam energy when it is in the T^* as opposed to T^{**} charge state. This is consistent with the fact that the T^* charge state is a stronger trapping center relative to the T^{**} charge state. Therefore, the probe beam in final steady state measures a fraction of the T^* charge state, which is the predominant charge state of the defect center after excitation removal.

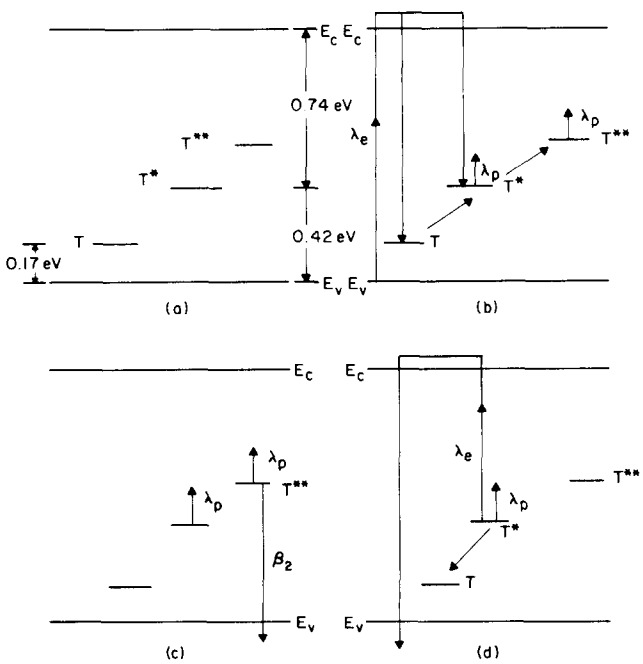

FIG. 8. Model of the HOB defect center for the bands studied (a) energy state, (b) the excitation process, (c) the decay process, and (d) depletion process.

It has been noted previously[8,9] and in the present study that the probe beam absorption does return to its original level when the excitation energy equal to the depletion energy is incident on the sample. The depletion process is characterized by the energy necessary to excite the electron of the T^* charge state to the conduction band, with subsequent decay to the valence band [Fig. 8(d)]. This energy value is essentially the distance of the defect level T^* from the con-

duction band edge and was experimentally determined to be 0.74 eV. When steady state is reached under depletion energy illumination, no additional absorption occurs because the defect centers are in the T charge state empty of electrons. At this point the probe absorption is once again at its original background value (i.e., without excitaton energy impressed on sample).

B. Comparison with photoluminescence studies

Radiation-induced defects in silicon have been studied using low temperature photoluminescence as the probe. In particular, photoluminescence studies in neutron-irradiated Si have been reported by Mudryi and Yukhnevich[12] and Tkachev and Mudri[13] while Noonan, Kirkpatrick, and Streetman[14] have studied the photoluminescence arising from defects introduced by 120-keV boron ion irradiation of silicon. Detailed annealing experiments on the defect states which produce photoluminescence have been reported.[12–14] Tkachev and Mudryi[13] have reported photoluminescence peaks of energy 1.0399, 1.0186, 1.0037, and 0.988 eV which only appear in neutron-irradiated silicon after annealing the sample for $\sim$20 min at temperatures in the range 300–550 °C. They[13] give as a possible interpretation for the first two peaks a defect consisting of 3–5 vacancies, while the latter two peaks are interpreted as possibly containing oxygen and carbon atoms as constituents of the defects. The significant point we can make is that the state T which we place near $\sim E_v + 0.17$ eV (see Fig. 1) could be the final state to which the electron decays and emits photoluminescence of one of the four peaks just stated above. In addition Tkachev and Mudryi[14] report photoluminescence peaks at 0.7667 and 0.7610 eV which only appear after annealing the sample for $\sim$20 min in the 325–550 °C temperature range. For these two peaks the state we show in Fig. 1 at charge state T^* ($E_v + 0.42$ eV) may be the final state to which the electron decays hence giving rise to the two just mentioned photoluminescence peaks. It is recognized that the conclusions relating photoluminescence peaks with HOB states is based on indirect experimental evidence.

In summary, the conclusions relating the identification of photoluminescence peaks with the HOB states we show at T and T^* is based on several similar properties of the defects: first, the defects are neutron induced, second they only appear after annealing for $\sim$20 min at temperatures in the range 300–500 °C and finally the positions of the HOB energy states T, T^* correlate with the photoluminescence peaks.[14] It is interesting to note that an optical center found in irradiated Si at 0.97 eV has been studied by photoluminescence[15–18] and the origin of this peak was recently reported by O'Donnell, Lee, and Watkins[19] using optical detection of magnetic resonance measurements. They[19] find the defect responsible for the 0.97-eV level to consist of two carbon atoms and an interstitial silicon atom such that the defect is in a positive charge state. Detailed annealing experiments[20] indicate the defect anneals completely in the 250–300 °C temperature range. Thus, the 0.97-eV photoluminescence peak is not associated with any defect which gives rise to the HOB studied in this paper. Finally, the photoluminescence peaks we identify with the HOB are not observed in electron irradiated Si.

C. Comparison with stress symmetry studies

We have performed studies on the response of HOB to uniaxial compressive stress.[7,8] For convenience we show in Fig. 9 the response to stress of each HOB studied earlier. As can be seen in Fig. 9 the 1048- and 1075-cm^{-1} bands and the 970- and 1101-cm^{-1} bands exhibit very nearly the same response to stress indicative of two defects having two different symmetries. The relative capture cross sections versus excitation energy given in Figs. 2 and 3 indicate that the 1048- and 1075-cm^{-1} bands and the 970- and 1101-cm^{-1} bands have roughly similar capture cross section versus excitation energy dependence. Note that the value of cross section at the peaks are nearly equal for the two bands at 1048 and 1075 cm^{-1}, while only the shapes are similar for the 970- and 1101-cm^{-1} bands. Thus, it can be argued that the HOB are due to two defects of different symmetry and that the defects exhibit at least two different responses to photoexcitation. However, the dependence of excitation τ_e^1 and decay τ_d^1 time constants on excitation energy for the 1048- and 1075-cm^{-1} bands and the 970- and 1101-cm^{-1} bands do not show a simple correlation (see Figs. 5 and 6), whereas the temperature dependence shown in Fig. 7 was typical of the HOB studied.

It was not possible to classify all the HOB with the ideal stress splitting patterns given by Kaplyanskii.[21] The stress data of Fig. 9 can be best fit in terms of treating the observed patterns as belonging to two defect symmetry groups: (1) tetragonal and (2) rhombic 1. Additional details on the symmetry properties and comparison to electron spin resonance studies on the defects giving rise to the HOB can be found elsewhere.[7,8]

A calculation of the photoexcitation electron capture cross section for the HOB bands following the methods outlined by Lang *et al.*[22] has been given elsewhere.[10] The main result of the calculation is that the electron capture cross

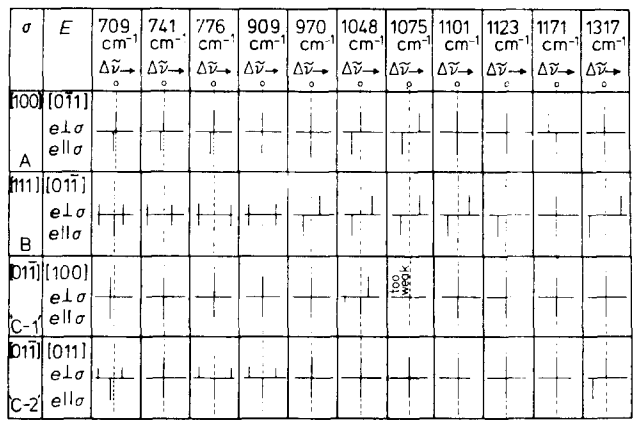

FIG. 9. Stress response of HOB at 78 K. σ is the stress direction, E the electric field intensity with polarization direction $e \perp$ or $\parallel$ to σ, $\Delta\tilde{\nu}$ represents the magnitude of the splitting or shift (in cm^{-1}) of the absorption peak from the unstressed state shown as the vertical dotted line marked with 0 at top of each column.

sections for the defects giving rise to the HOB are factors of 10^3–10^5 times smaller than the photoionization cross sections measured for gold acceptor impurities in silicon.[22] This simple calculation indicates that chemical impurity defects such as Au must have a high affinity for photoionization whereas the capture process of photoexcited electrons to HOB defects occurs with a very low probability by comparison to Au in Si.

Finally, we conclude that the defects which are responsible for HOB arise from the redistribution by heat treatment of simple defects such as divacancies, interstitials, etc. Thus, basic simple defects are precursors of the more complex defects associated with HOB's in both neutron and ion-irradiated Si. The HOB's represent the optical activity associated with dangling bonds of point defects just before the final bond arrangements are made after high temperature annealing such as proposed by Tan.[23]

ACKNOWLEDGMENTS

The authors thank the late John W. Cleland of Oak Ridge National Laboratory for providing the irradiated silicon samples. We also thank Dr. James W. Corbett of SUNY/Albany for discussions on improving some aspects of our experimental methods. Finally, we acknowledge the financial support of this research by the National Science Foundation.

[1]J. C. Corelli, R. C. Young, and C. S. Chen, IEEE Trans. Nucl. Sci. **NS-17**, 126 (1970).
[2]M. T. Lappo and V. D. Tkachev, Sov. Phys. Semicond. **5**, 1411 (1972).
[3]C. S. Chen, R. Vogt-Lowell, and J. C. Corelli, *Radiation Damage and Defects in Semiconductors*, (Institute of Physics, London, 1973) IOP Conf. Ser. Vol. 16, p. 210.
[4]Y. P. Koval, V. N. Mordkovich, E. M. Temper, and V. A. Kharchenko Sov. Phys. Semicond. **6**, 1152 (1973).
[5]V. N. Mordkovich, S. P. Solov'ev, E. M. Temper, and V. A. Kharchenko, Sov. Phys. Semicond. **8**, 666 (1974).
[6]R. C. Newman and D. H. J. Totterdell, J. Phys. C **8**, 3944 (1975).
[7]J. C. Corelli, D. Mills, R. Gruver, D. Cuddeback, Y. H. Lee, and J. W. Corbett, *Radiation Effects in Semiconductors 1976*, edited by N. B. Urli and J. W. Corbett (Institute of Physics, London, 1977) IOP Conf. Ser. Vol. 31 p. 251.
[8]J. C. Corelli and J. W. Corbett, *Neutron Transmutation Doped Silicon*, edited by J. Gulberg (Plenum, New York, 1981), p. 35.
[9]M. T. Mitchell, J. C. Corelli, and J. W. Corbett, *Defects and Radiation Effects in Semiconductors, 1978*, edited by J. H. Albany (Institute of Physics, Bristol, 1979) IOP Conf. Series Vol. 46, p. 317.
[10]W. Vidinski, J. C. Corelli, and A. J. Steckl, J. Nucl. Mater. **108 & 109**, 693 (1982).
[11]J. Tauc, *International Conference on the Physics of Semiconductors* (Institute of Physics and the Physical Society, London, 1962), pp. 333–334.
[12]A. V. Mydryi and A. V. Yukhnevich, Sov. Phys. Semicond. **7**, 117 (1973).
[13]V. D. Tkachev and A. V. Mudryi, *Radiation Effects in Semiconductors, 1976*, edited by N. B. Urli and J. W. Corbett (Institute of Physics, London, 1977) IOP Conference Series Vol. 31, p.231.
[14]J. R. Noonan, C. G. Kirkpatrick, and B. G. Streetman, Radiat. Eff. **21**, 225 (1974).
[15]A. V. Yuknevich, Sov. Phys. Solid State **1**, 259 (1965).
[16]A. R. Bean, R. C. Newman, and R. S. Smith, J. Phys. Chem. Solids **31**, 739 (1970).
[17]A. V. Yuknevich and A. V. Mudryi, Sov. Phys. Semicond. **7**, 815 (1973).
[18]J. R. Noonan, C. G. Kirkpatrick, and B. G. Streetman, J. Appl. Phys. **47**, 3010 (1976).
[19]K. P. O'Donnell, K. M. Lee, and G. D. Watkins, 12th International Conference on Defects in Semiconductors Amsterdam, Sept. 1982 (to be published).
[20]V. S. Konoplev, A. A. Gippius, and V. S. Vavilov, *Radiation Effects in Semiconductors* 1976, edited by N. B. Urli and J. W. Corbett (Institute of Physics, London, 1977) IOP Conference Series Vol. 31, p. 244.
[21]A. A. Kaplyanskii, J. Phys. Paris Coll. Suppl. 8-9, **28** C4-39 (1967).
[22]D. V. Lang, H. G. Grimmeiss, E. Meijer, and M. Jaros, Phys. Rev. B **22**, 3917 (1980).
[23]T. Y. Tan, *Defects in Semiconductors Vol. 2*, edited by J. Narayan and T. Y. Tan (North Holland, New York, 1981) pp. 163–172.